6 Use of Double Barrel Micropipettes to Voltage-Clamp Plant and Fungal Cells

ROGER R. LEW

6.1 Intracellular measurements in intact, turgid cell compared with protoplasts

In a paper published in 1977, Racusen et al. documented a startling property of higher plant cells: The membrane potential of a higher plant cell responds to the extracellular osmolarity, depolarizing under hyper-osmotic treatment, up to and including the point of plasmolysis. The effect was reversed by removing the extracellular osmoticum. Isolated protoplasts exhibited very depolarized potentials compared with intact turgid cells. Osmotic effects on the electrical properties extend beyond changes in the membrane potential. The conductance, a measure of the voltage dependence of ionic current flow across the plasma membrane, also changes in response to either hyper- or hypo-osmotic treatment (Lew 1996). Indeed, at least in *Arabidopsis thaliana* the electrical changes coincide with changes in the net ionic fluxes that contribute to turgor recovery after hyperosmotic treatment (Shabala and Lew 2002). These electrical changes are an important part of the cell's response to osmotic stresses, but their significance is even greater, because of the implications for the use of patch clamp to measure ionic properties of plant and fungal cells.

6.1.1 Protoplasts are required for patch clamp

Patch clamp (Hamill et al. 1981) revolutionized the study of ion transport in cells, including animal, fungal, algal and higher plant cells. The two major discoverers, Erwin Neher and Bert Sakmann, were awarded the Nobel Prize in 1991. The power of the patch clamp technique was 2-fold. First, it allowed individual ion channels to be measured in situ, in their natural states in the membrane. Second, with the whole cell mode, it enabled the experimenter to extend the range of possible measurements: to examine the voltage and time dependence of ionic currents and use this information to identify the specific ions contributing to the current. With patch clamp, a wealth of information has been uncovered about the molecular foundations of ionic transport in

York University, Department of Biology, Toronto, Ontario M3J 1P3, Canada

Plant Electrophysiology – Theory & Methods (ed. by Volkov)

cells. However, when the patch clamp technique is applied to walled cells, the wall must first be removed to expose the plasma membrane to the patch pipette. To avoid lysis, the cell must be held in a solution of osmolarity high enough to induce plasmolysis. This is necessary whether the wall is removed by enzymatic digestion or some other technique, such as laser ablation. This means that the advantage of patch clamp, to examine the voltage and time dependence of ion transport across the plasma membrane, is offset by the non-physiological condition of the cell, plasmolyzed and probably attempting turgor recovery. Certainly not growing, certainly in an abnormal physiological state, the plasmolyzed state of the cell is a technical problem that obscures the relevance of patch clamp measurements. The ideal way to overcome this is to perform measurements of the voltage and time dependence of ionic currents in intact, turgid, possibly even growing cells. But how can this be done in an intact cell?

6.2 Voltage clamping intact turgid cells

Voltage clamp is the technique of choice to measure the voltage and time dependence of ionic currents across the plasma membrane. In essence, the electronics are designed to inject a current sufficient to maintain the voltage of the plasma membrane at a specified level. Data for a number of different clamped voltages are compiled to create a current versus voltage relation, or current is monitored at a single voltage over time to measure time dependence, or both may be combined. It is useful to measure the cell membrane potential concurrent with current injection into the cell to confirm the fidelity of voltage clamping. There are three ways to voltage clamp intact turgid cells: discontinuous voltage clamp, dual impalements, and double barrel micropipettes. In all instances, the intent is to measure the voltage and time dependence of the plasma membrane ionic currents separate from any contribution of the micropipette itself. The micropipette resistance is a significant problem, because the resistance at the tip of the micropipette is often similar in magnitude to the resistance of the plasma membrane. This can cause an inability to separate the voltage and time dependence of ionic currents through the micropipette tip from the ionic currents through the plasma membrane.

6.2.1 Discontinuous voltage clamp: a single barrel used for both current injection and voltage monitoring

Finkel and Redman (1984) described the discontinuous single microelectrode voltage clamp technique. The technique has been used successfully in intact higher plant cells. The basic idea is that the time dependence of electrical currents at the microelectrode tip is very different from those of the plasma membrane because the capacitance of the micropipette tip is much lower

than the capacitance of the cell membrane. This will cause a much faster time response, τ, defined as resistance (R) $\times$ capacitance (C): $\tau = R \times C$. By rapidly switching between current injection and voltage measurements, it is possible to separate *temporally* the contribution of the micropipette from the contribution of the plasma membrane, as long as $\tau_{electrode} < \tau_{cell}$. A set of papers using the discontinuous single electrode voltage clamp technique illustrates the technique and problems. Forestier et al. (1998) explored the use of the technique to identify slow anion currents in guard cells. The advantage of the technique was that measurements could be done in intact cells. Since guard cells are turgor-active, that is, change their turgor in response to different stimuli to control stomata aperture in the epidermis of the leaf, intact cells offer much greater insight into ion transport required for turgor changes compared to the turgor-less protoplasts necessary for patch clamp. In the discontinuous single electrode voltage clamp technique, it is necessary to compensate electronically for the capacitance of the electrode. Roelfsema et al. (2001) raised doubts about the applicability of the discontinuous single-electrode voltage clamp technique in small cells, such as guard cells, because the low capacitance of small cells would be similar to the capacitance of the electrode ($\tau_{electrode} \sim \tau_{cell}$); thus, a clear separation of the contribution of the electrode and cell would be difficult. Raschke et al. (2003) confirmed the results of Forestier et al. (1998), noting that it is crucial to use micropipettes which possess a linear current-voltage relation to assure that their capacitance can be compensated electronically. That is, the resistance must be voltage independent to assure $R \times C$ is constant for all clamped voltages. Although others have used this technique, the three papers cited above give a flavor of the doubts associated with the method. There are two issues: whether it is electronically possible to compensate for the electrode capacitance (or more accurately, time response, $R \times C$) consistently, and whether the properties of the microelectrode tip are the same before and during insertion into the cell. In fact, Etherton et al. (1977) explored the latter question by directly comparing membrane resistance measurements obtained using two electrodes impaled separately into the same cell with single electrode impalements. They expressed the concern that the properties of the single electrode change upon impalement, rendering the technique questionable. Guard cells do not lend themselves to multiple impalements, so the discontinuous voltage clamp technique remains a useful technique to avoid the protoplasting required to patch clamp the cell, with caveats regarding the quality of the data. Supporting evidence, such as inhibitor effects (Forestier et al. 1998; Bouteau et al. 1999), bolsters interpretation of the data.

6.2.2 Dual impalements

Etherton et al. (1977) assumed that dual impalements with a voltage monitoring electrode and a current-injecting electrode were the "standard by which the accuracy" of single electrode techniques "could be judged". Since

the two processes, voltage monitoring and current injection, are separate, this is a likely assumption. One concern exists, that multiple impalements may affect the resistance of the plasma membrane due to membrane damage caused by the impalements, but Lew (2000) presented evidence discounting this possibility, at least in root hairs, by showing that multiple impalements do not cause a decrease in the potential, expected if the impalement site is the site of significant ionic leakage. Multiple impalements are technically difficult. The cells must be accessible, and good imaging is very helpful, to ensure the micropipettes are impaled into the same cellular compartment. Indeed, the "standard" to identify where the tips are located is fluorescent dye injection (Holdaway-Clarke et al. 1996). Because only a single impalement into the cell is required, double barrel micropipettes offer technical advantages, while retaining separation of the voltage and current-injecting microelectrodes.

6.2.3 Double barrel micropipettes

A number of researchers have used double barrel micropipettes over the years. Michael Blatt and others used them to perform voltage clamping of the filamentous fungus *Neurospora crassa* (Blatt and Slayman 1983, 1987). Blatt subsequently used the technique in guard cells (Blatt 1987), and wrote a primer on double barrel micropipettes and other electrophysiological techniques (Blatt 1991) which I recommend highly for new and experienced electrophysiologists.

6.3 Double barrel micropipette fabrication

The fabrication of double barrel micropipettes involves a sequential set of steps that are best performed by fabricating a batch of micropipettes at the same time. Borosilicate capillaries with internal filaments are first cut to an appropriate length (about 7 cm). We use 1 mm OD, 0.58 mm ID tubing. The two capillaries are inserted into a micropipette puller in which one of the two clamps on either side of the heating filament can be rotated (Fig. 6.1). When the heating filament has softened the glass, the capillaries are rotated by 360° to create a twist in the glass. Then standard pulling protocols are used to pull the micropipette. Once pulled, a small amount of fast-setting epoxy is applied just above the twist to strengthen the fused joint between the two capillaries. Finally, one of the barrels is heated and pulled away to form a Y-shape. This eases insertion of one of the barrels of the micropipette into a holder, and insertion of a chlorided silver wire into the other barrel. Photographs of some of the fabrication steps are shown in Fig. 6.2.

Typically, we fabricate eight to ten of the double barrel micropipettes at the same time, First, all are pulled. Then epoxy is applied. When hardened,

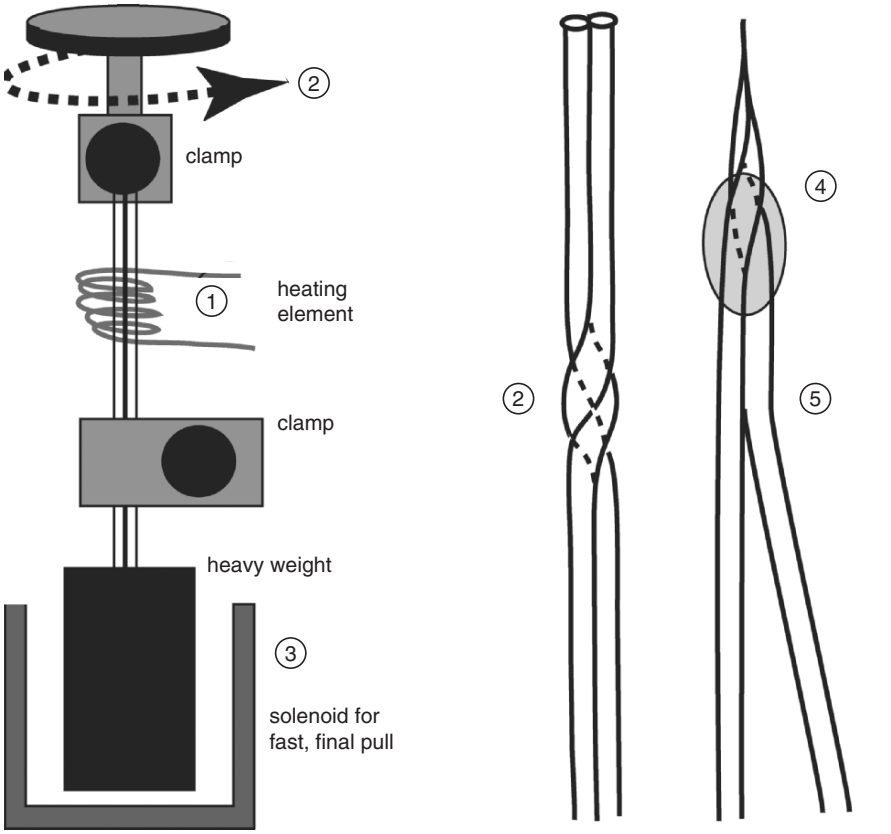

Fig. 6.1. Construction of a double barrel micropipette. Step 1: heat two capillaries held together in clamps above and below a heating element which heats the two capillaries in a localized region. Step 2: when the glass has softened, the two capillaries are twisted by rotating one of the clamps 360°. Step 3: the two capillaries are pulled to form the sharp tip, and removed from the pipette puller. Step 4: a drop of fast-setting epoxy is applied to the joint between the two barrels at the fused twist to strengthen the joint. Step 5: one of the capillaries is softened by localized heating and pulled away to produce a Y-shape

one barrel is pulled away to form a Y. Then they are stored in a covered dish until used. Fabrication takes about 1–2 h.

One problem that can arise is crack formation in one of the glass barrels, probably during the twisting if the glass has not softened enough during heating. The cracks are not visible (except as a stress crack under magnification), but reveal themselves when the micropipettes are being tested for tip resistance and crosstalk just prior to impalements. At this time, the crack causes an extremely low resistance in one of the barrels, far less than the 20 MΩ norm.

Filling of the micropipette barrels with electrolyte is done as with a single barrel electrode. Usually, a small amount of electrolyte is injected into the

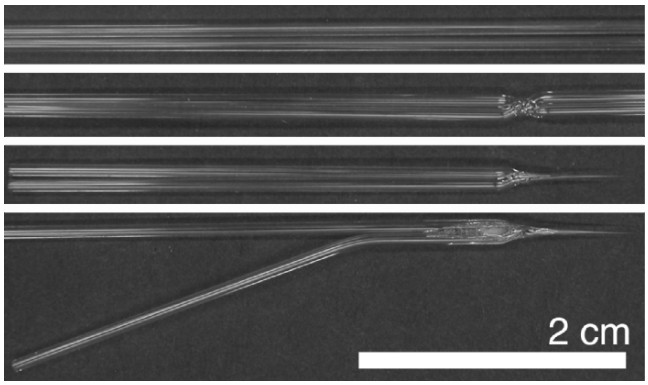

Fig. 6.2. Stages in the construction of a double barrel micropipette. The *upper panel* shows the two capillaries, twisted together in the *second panel*, pulled in the *third panel*, and after final fabrication in the *fourth panel*. Bar=2 cm

blunt end of capillaries; 10 min later, the tip will have filled due to capillary action because of the internal filament. Even the glass twist will have filled. Backfilling of the bent barrel requires a fine gauge needle, so that it can be easily inserted past the bend right up to the twist.

6.3.1 Limitations

There are limitations to the use of double barrel micropipettes due to crosstalk and the localized nature of the current injection and voltage monitoring

6.3.1.1 Crosstalk between barrels

In a double barrel micropipette, the glass wall separating the two barrels is twice the thickness of the outer glass walls (Fig. 6.3). However, it is possible that some current will "leak" across the wall. The response of both barrels to a current injected through one barrel is shown in Fig. 6.4. There are voltage deflections in the second barrel. Initially, there is a capacitance spike due to capacitative coupling between the two barrels, followed by a steady state deflection of very small magnitude. The deflection, expressed as percent coupling $[100 \times (\Delta E_2/\Delta E_1)]$, is about 1–2%.

6.3.1.2 Maximal current injection

As a consequence of the crosstalk between the two barrels, double barrel micropipettes are not suitable for measurements requiring large current injections. A 2 nA current causes a very small voltage deflection in the second

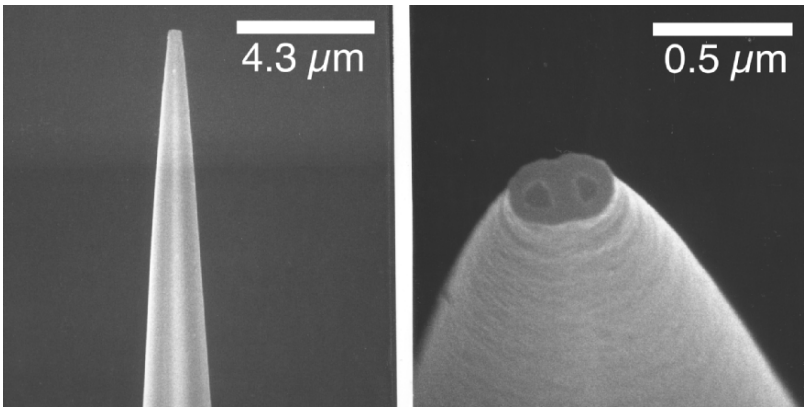

Fig. 6.3. Scanning electron microscopy of double barrel micropipette tip. The *left panel* shows the tip shape. The *right panel* shows the tip apertures. Note the double thickness of glass between the two apertures. Bars 4.3 and 0.5 μm, as shown

barrel, but a μA current will cause a deflection large enough to affect measurements in walled cells, whose membrane potentials range from –50 to –200 mV. Thus, double-barrel micropipettes are not suitable for measurements where μA currents are required, such as the green algae *Chara* and *Nitella*, although larger micropipette apertures may be a solution.

6.3.1.3 Space clamping

Another problem associated with large cells is the incomplete "spread" of voltage throughout the cell. When voltage clamping, the cell may not attain the specified voltage, this is incomplete space clamping. It is a problem for double barrel microelectrodes, because current injection and voltage monitoring occur in the same region within the cell. Incomplete space clamping should not be a problem for small, electrically isolated cells (such as guard cells). However, with large cells, or when there is electrical coupling between cells, the problem is pervasive. Under these conditions, quantitation requires multiple impalements, and correction depends upon assumptions about current spread and cell geometry. There is no simple authoritative solution. Examples of space clamping problems are shown for different cell types later in the chapter.

6.4 Use: electronics and computer control

There are many resources describing electronics and computer control of experiments. Purves (1981) is a classic, still timely today. Ogden (1994) includes very useful contributions on microelectrodes, voltage clamping

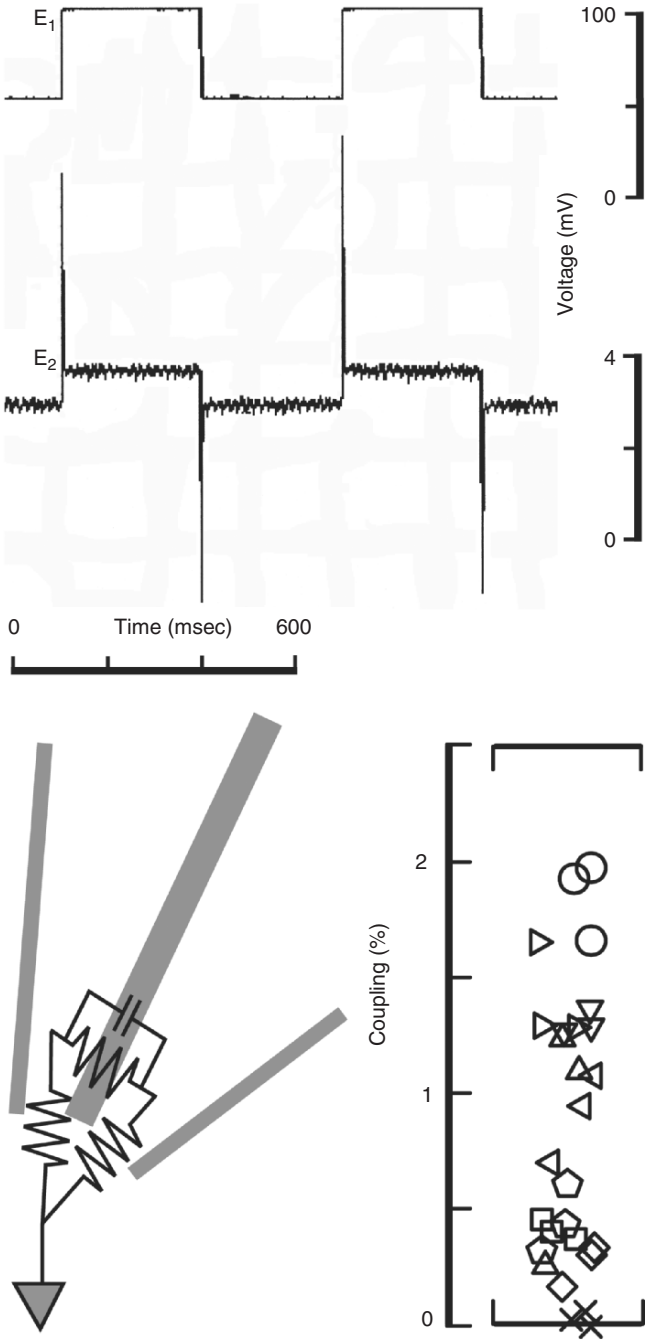

Fig. 6.4. Electrical properties of the double barrel micropipette. The upper panel shows the voltage response of the two barrels (E_1 and E_2) to a 2 nA peak to peak current injected into the first barrel (E_1). The large voltage deflection in the first barrel causes a large voltage deflection

techniques and computer control. For versatility, digital oscilloscopes are used to monitor experiments and print a copy of recordings. For computer control, we use analog/digital converters for measuring voltage and clamping currents, digital/analog converters for controlling the clamped voltage, digital input/output to switch voltage clamping on, and timers to control the duration of the voltage clamp; all are supplied by a Labmaster board from Scientific Solutions (Solon, Ohio, USA). The required software is written in C, compiled and run on a DOS computer. While this may seem anachronistic, the advantage for us is complete control of the experimental environment, including the CPU cycles of the computer. The technical specifications for hardware control have not changed, so newer systems offer little advantage. For new or experienced electrophysiologists, writing the software programs may be too daunting. If this is so, turnkey systems are available from many vendors at a significant cost. The latest development is the inclusion of a DSP (digital signal processor) chip in a stand alone system for performing measurements and voltage clamp.

6.4.1 Electrometers and voltage clamp circuit

Any electrometer with a sufficiently high input impedance ($>10^{11}$ Ω) will work. It is important to assure that the time responses of the voltage and current injecting headstages are the same, thus the input impedances should be matched. A voltage clamp circuit is connected to the electrometers. A schematic of the electronic circuit is shown in Fig. 6.5.

6.5 Examples of measurements

Examples of measurements in walled cells can include any situation where current injection and voltage measurements must be kept separate. It is important to emphasize that like any technique, double barrel micropipettes

---

Fig. 6.4. (*Continued*) due to the resistance of the micropipette tip, 25 MΩ in this example. Some of the current "leaks" across the glass barrier between the two barrels, causing a much smaller voltage deflection in the second barrel (E_2, about 1 mV). Note that there is a spike at each step transition in the current injection, caused by the capacitance of the glass barrier between the two barrels. The measurements were performed with 3 M KCl filling the barrels, and 150 mM KCl in the external solution to mimic the ionic conductivity of the cytoplasm. Grounding was performed using a chlorided silver wire (no agar salt bridge was used to minimize stray resistance that would cause a larger voltage deflection in E_2). The resistive network is shown in the lower left panel. By measuring the resistance of each barrel, and the amount of 'coupling' between the barrels ($100 \times (\Delta E_2/\Delta E_1)$) (shown in the *lower right panel*, data are jittered for clarity), it was possible to estimate the value of the resistance of the glass barrier between the two barrels. The value ranged from 500 MΩ to 100 GΩ, the median value was 3 GΩ. This is consistent with the known resistivity of borosilicate glass, about 10^{15} Ω × cm. With an estimated barrier thickness of 100 nm, the calculated resistance would be 10 GΩ

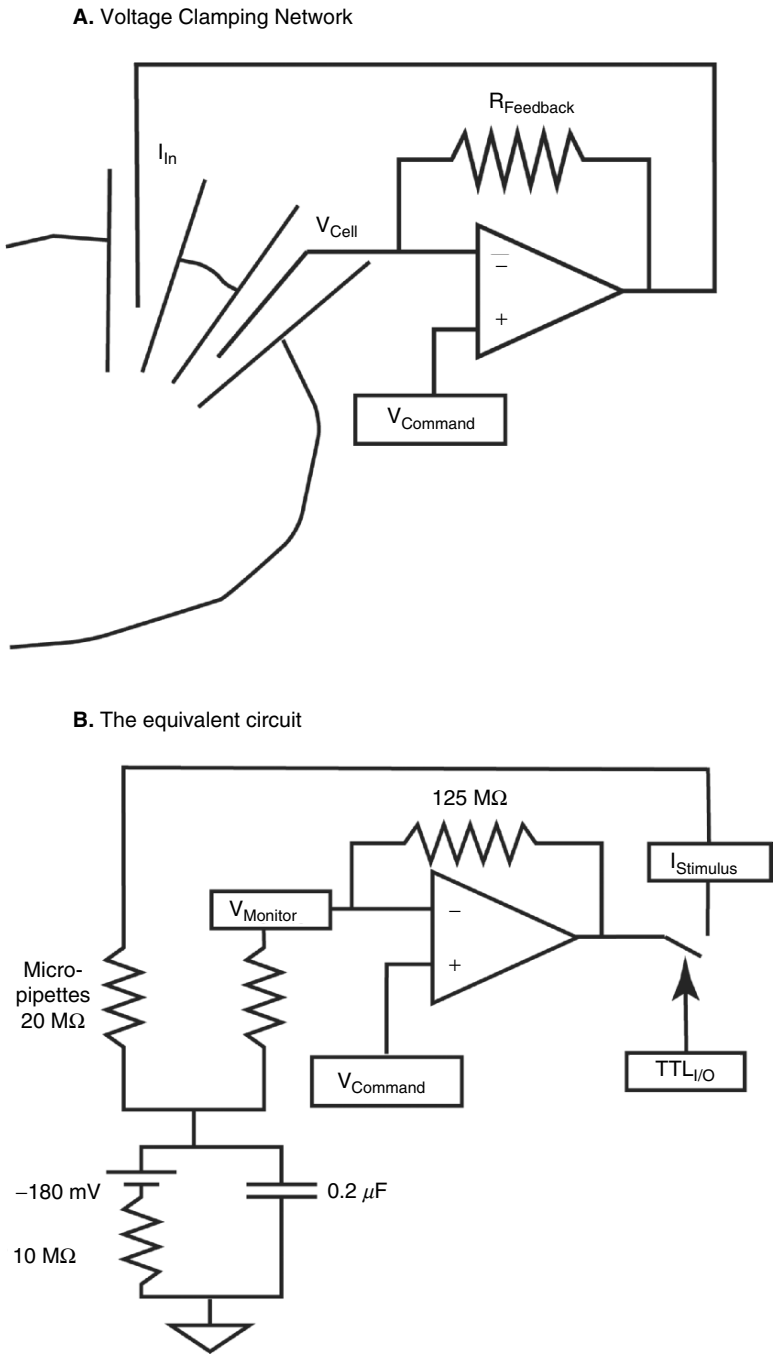

Fig. 6.5. Voltage clamping schematic. **A** If we specify $V_{Command}$, the operational amplifier will drive whatever current is necessary into the feedback system (the cell and feedback resistor $R_{Feedback}$) to maintain V_{Cell} at $V_{Command}$. **B** A more detailed equivalent circuit. The $TTL_{I/O}$ is a switch relay

may not be sufficient to resolve the electrical properties of a cell. Some of these issues are outlined in the following examples.

6.5.1 Input resistance

By injecting a known current through one barrel, the magnitude of the voltage deflection in the other barrel can be used to calculate the resistance of the cell. If the geometry of the cell is known, than the specific resistance can be calculated. An example of a measurement is shown in Fig. 6.6. The example is from

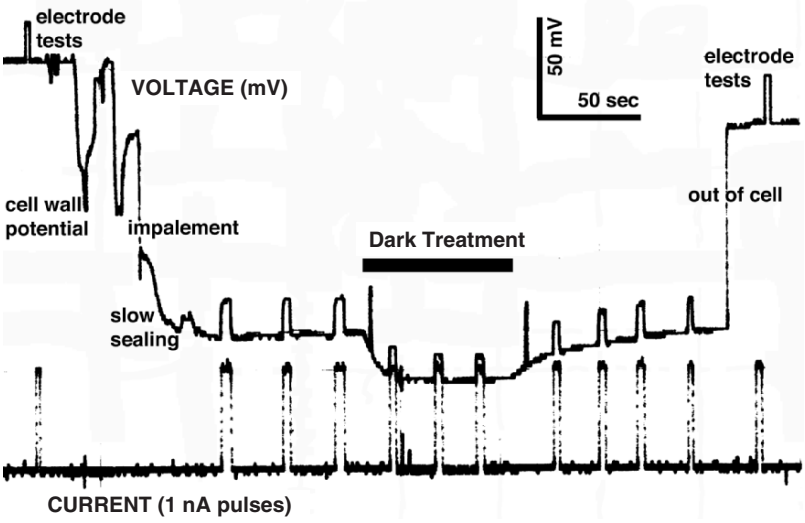

Fig. 6.6. Example of input resistance measurements from a mesophyll cell of *Ceratopteris richardii*. Both voltage (*top trace*) monitored with one barrel of the double barrel micropipette and current (*lower trace*) injected through the other barrel are shown. Prior to and after the experiment, electrode tests were conducted to assure there was no electrical crosstalk between the voltage monitoring and current injecting electrodes. Current injection through the voltage-monitoring electrode causes a voltage deflection as expected, but current injection through the current-injecting electrode caused no visible deflection in the voltage-monitoring electrode. Immediately following impalement, confirmed visually, a transient negative spike is followed by a slow sealing event that is characterized by a gradual hyperpolarization to a stable potential. After impalement, current injection through one barrel of the double barrel micropipette causes a voltage deflection in the other barrel due to the resistance of the plasma membrane. This confirmed that the impalement was successful. The response of the cell to changes in photosynthesis are documented in this experiment. Removal of the pipette from the cell results in a rapid depolarization to a value similar to what was observed before the cell was impaled

Fig. 6.5. (*Continued*) controlled by the computer to turn on the voltage clamping circuit. The V_{Cell} is measured at the electrometer ($V_{Monitor}$). The current is injected via the $I_{Stimulus}$ input of another electrometer. The feedback resistor in this example is very high (125 MΩ) and assures a fast response by the operational amplifier so that V_{Cell} is rapidly clamped with high fidelity

a mesophyll cell of a *Ceratopteris richardii* gametophyte. In these cells, dye injected into the cell was distributed throughout the cytoplasm and did not migrate into adjacent cells, indicating that the impalement was cytoplasmic, and that cell-to-cell coupling was minimal. Having measured the mesophyll cell dimensions, the specific resistance could be calculated: about 1.5 $k\Omega \times cm^2$.

6.5.2 Current–voltage relations

An example of a current-voltage measurement using voltage clamping is shown in Fig. 6.7, using trunk hyphae of the fungus *Neurospora crassa*. The measurement illustrates not only the voltage clamp technique, but also the issue of space clamping. A hyphal compartment was impaled with a double barrel micropipette, and an adjacent compartment (separated from the first by a septal pore) was impaled with a single barrel micropipette. Although voltage fidelity was observed for the voltage clamp in the first compartment, current leakage through the plasma membrane causes an attenuated voltage clamp in the second compartment. As a result, the clamping current overestimates the "real" clamping current in the first compartment. Cable theory can be used to correct for current attenuation in fungal hyphae (Gradmann et al. 1978).

6.5.3 Cell-to-cell coupling

An example of the use of double barrel micropipettes to measure electrical coupling through plasmodesmata is shown in Fig. 6.8. The example is adjacent root hairs on an *Arabidopsis thaliana* root. Analogous to fungal hyphae, electrical connections between cells results in significant current passage into adjacent cells, resulting in an overestimate of the clamping current in voltage clamp measurements.

6.6 Summary

Electrophysiological analyses of ion transport in walled cells are essential to our understanding of the life of the cell. Ion transport plays crucial roles in regulating the intracellular milieu of the cell, in signal transduction, osmotic regulation and cellular growth. A detailed characterization of the electrical properties of the cells relies upon multiple techniques, among them, voltage clamping is very useful. Voltage clamping with double barrel micropipettes is especially important given the "physiology problem" associated with patch clamp measurements on plasmolyzed protoplasts. Technical constraints and accessibility of the cell make voltage clamping a challenging endeavor, but

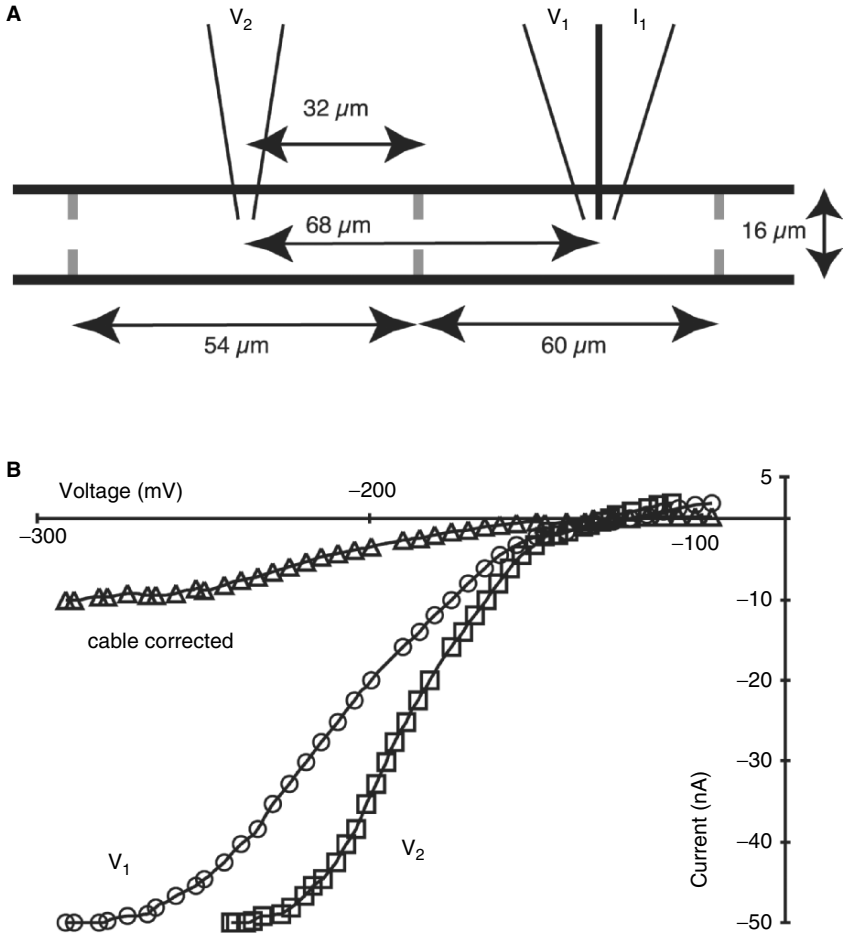

Fig. 6.7. Current–voltage measurement. The example is for a hyphal trunk of the fungus *Neurospora crassa*. A schematic of the two impalements, and hyphal geometry are shown in **A**. Note the presence of septal pores, which allow for the free movement of cytoplasm between each hyphal "cell" unit. Voltage clamping using the V_1 and I_1 microelectrodes was for the range –300 to –100 mV. The clamp duration was 50 ms, the voltage at V_1 and V_2, and the clamping current (I_1) were obtained by averaging the last five data samples before the end of the clamp. Note that the *real* voltages, rather than the computer specified clamped voltage were measured. Because of current attenuation as it passes along the hypha, the voltage at V_2 was less than the voltage at V_1. Thus space clamping was incomplete. To correct for current attenuation, the equation $I_m = I \times ln(\Delta V_1/\Delta V_2)$ was used (Rall 1977), where I is the total current, I_m is the cable corrected current, ΔV_1 is the clamped voltage minus the resting potential at V_1, and ΔV_2 is the clamped voltage minus the resting potential at V_2. The current density, A cm^{-1} can be calculated from $I_m/(2 \times \Delta x)$, where Δx is the distance between the two electrodes (68 μm in this example), and yields values in the range –0.74 to 0.021 μA cm^{-1}

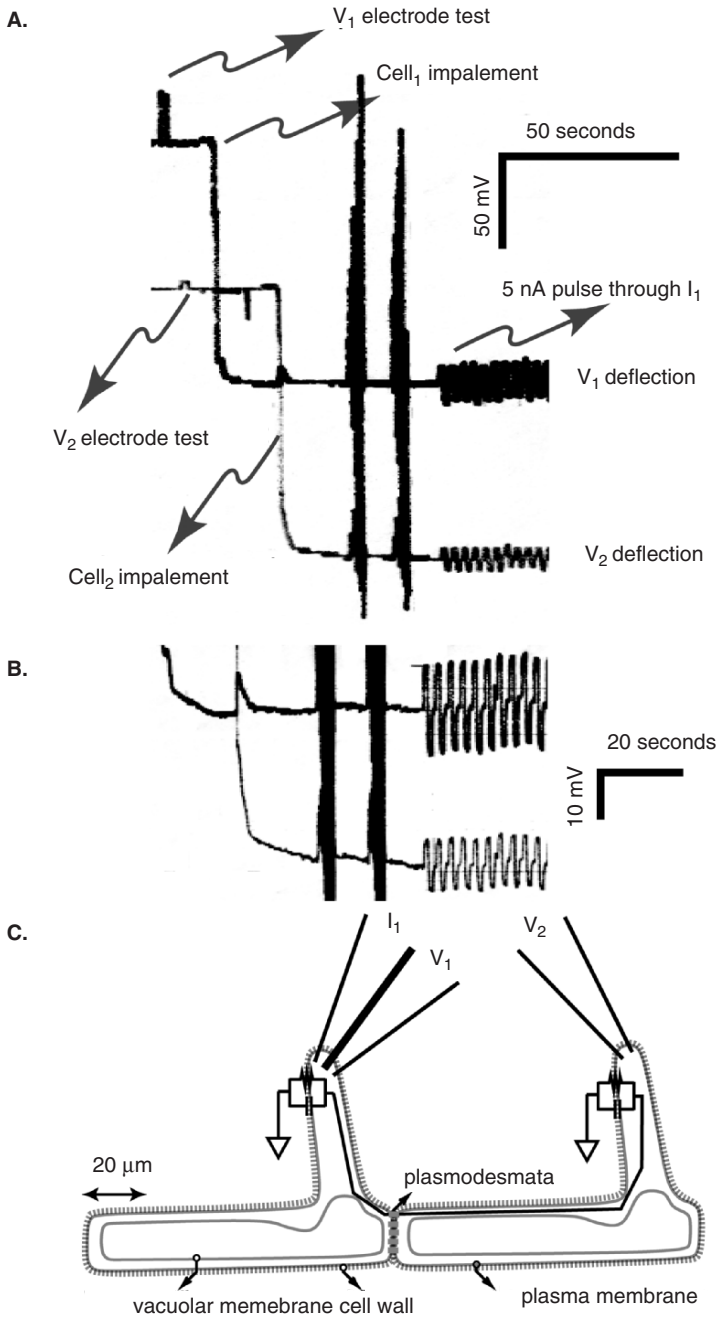

Fig. 6.8. Example of cell-to-cell coupling measurement. This example is for two root hairs adjacent to each other on a longitudinal file of an *Arabidopsis thaliana* root. **A** As marked, $cell_1$ is impaled with a double-barrel electrode, followed by a separate impalement into $cell_2$. A 5 nA

pulse through the current-injecting electrode in $cell_1$ results in a voltage deflection in both $cell_1$ and in $cell_2$, due to coupling through plasmodesmata. **B** A higher magnification segment of the traces shown in **A. C** A diagrammatic representation of cell-to-cell coupling through plasmodesmata. Regulation of cell-to-cell coupling between root hairs was described by Lew (1994)

double barrel micropipettes offer increased technical ease, simplifying the challenges faced by the researcher when working with intact cells. However, it should be clear from the examples presented in this chapter that double barrel micropipettes are not an absolute solution, but instead another step in our efforts to discover the roles of ion transport in cellular functions.

References

Blatt MR (1987) Electrical characteristics of stomatal guard cells: the ionic basis of the membrane potential and the consequence of potassium chloride leakage from microelectrodes. Planta 170:272–287

Blatt MR (1991) A primer in plant electrophysiological methods. In: Hostettmann K (ed) Methods in plant biochemistry, vol 6. Assays for bioactivity. Academic Press, London (xi and 360 pp), pp 281–321 (ISBN: 0124610161)

Blatt MR, Slayman CL (1983) KCl leakage from microelectrodes and its impact on the membrane parameters of a nonexcitable cell. J Membr Biol 72:223–234

Blatt MR, Slayman CL (1987) Role of "active" potassium transport in the regulation of cytoplasmic pH by nonanimal cells. Proc Natl Acad Sci USA 84:2737–2741

Bouteau F, Pennarun A-M, Kurkdjian A, Convert M, Cornel D, Monestiez M, Rona J-P, Bousquest U (1999) Ion channels of intact young root hairs from *Medicago sativa*. Plant Physiol Biochem 37:889–898

Etherton B, Keifer DW, Spanswick RM (1977) Comparison of three methods for measuring electrical resistances of plant cell membranes. Plant Physiol 60:684–688

Finkel AS, Redman S (1984) Theory and operation of a single microelectrode voltage clamp. J Neurosci Meth 11:101–127

Forestier C, Bouteau F, Leonhardt N, Vavasseur A (1998) Pharmacological properties of slow anion currents in intact guard cells of *Arabidopsis*. Application of the discontinuous single-electrode voltage-clamp to different species. Pflugers Arch 436:920–927

Gradmann D, Hansen U-P, Long WS, Slayman CL, Warncke J (1978) Current–voltage relationships for the plasma membrane and its principal electrogenic pump in *Neurospora crassa*: steady-state conditions. J Membr Biol 39:333–367

Hamill OP, Marty A, Neher E, Sakmann B, Sigworth FJ (1981) Improved patch-clamp techniques for high-resolution current recording from cells and cell-free membrane patches. Pflugers Arch 391:85–100

Holdaway-Clarke TL, Walker NA, Overall RL (1996) Measurement of the electrical resistance of plasmodesmata and membranes of corn suspension-culture cells. Planta 199:537–544

Lew RR (1994) Regulation of electrical coupling between *Arabidopsis* root hairs. Planta 193:67–73

Lew RR (1996) Pressure regulation of the electrical properties of growing *Arabidopsis thaliana* L. roothairs. Plant Physiol 112:1089–1100

Lew RR (2000) Electrobiology of root hairs. In: Ridge RW, Emons AMC (eds) Root hairs. Cell and molecular biology. Springer, Berlin Heidelberg New York, pp 115–139

Ogden D (ed) (1994) Microelectrode techniques. The Plymouth workshop handbook. The Company of Biologists, Cambridge, x + 448 pp

Purves RD (1981) Microelectrode methods for intracellular recording and ionophoresis. Academic Press, London, x + 146 pp

Racusen RH, Kinnersley AM, Galston AW (1977) Osmotically induced changes in electrical properties of plant protoplast membranes. Science 198:405–407

Rall W (1977) Core conductor theory and cable properties of neurons. In: Kandel ER (ed) Handbook of physiology, vol 1 (Cellular biology of neurons, part 1). American Physiological Society, Bethesda, pp 39–97

Raschke, K, Shabahang M, Wolf R (2003) The slow and the quick anion conductance in whole guard cells: their voltage-dependent alternation, and the modulation of their activities by abscisic acid and CO_2. Planta 217:639–650

Roelfsema, MRG, Steinmeyer R, Hedrich R (2001) Discontinuous single electrode voltage-clamp measurements: assessment of clamp accuracy in *Vicia faba* guard cells. J Exp Bot 52:1933–1939

Shabala S, Lew RR (2002) Turgor regulation in osmotically stressed *Arabidopsis thaliana* epidermal root cells: Direct support for the role of inorganic ion uptake as revealed by concurrent flux and cell turgor measurements. Plant Physiol 129:290–299